

SPILLOVER NOISE TEMPERATURE CALCULATIONS FOR THE
GREEN BANK CLEAR APERTURE ANTENNAS. Srikanth
October 4, 1989

INTRODUCTION:

There has been some discussion about the location of the subreflector and the arm that supports it with respect to the main reflector on the Green Bank clear aperture antenna. Locating the arm at the top of the dish as in Figure 1a (when the antenna is pointing horizon) seems prudent from points of view of structure and cost. But accessibility to the receiver cabin located in the arm becomes difficult. Accessibility could be improved by designing the antenna to travel past zenith by about 40° or so. If the support arm is at the bottom of the dish (Figure 1b), accessibility is no longer a problem. However, in this configuration additional steel may be required and the price of the antenna is likely to go up by about \$3M as per Lee. The spillover contribution to the system temperature could be quite different for the two cases. This memo is the result of an attempt to estimate the spillover temperature for both cassegrain and gregorian geometries with the subreflector either at the top or at the bottom.

COMPUTATION METHODOLOGY:

The noise contribution from beyond the edge of a reflector is due to two effects, namely spillover and diffraction by the edge. The first of the above two is the dominant contributor and only this effect is considered in this memo. The spillover in a dual reflector antenna has two components, (i) the feed spillover past the rim of the subreflector or forward spillover and (ii) spillover of the subreflector scattered radiation past the rim of the main reflector or rear spillover.

In the case of a symmetric antenna, the incident pattern on the sub/main reflector is almost always circularly symmetric. The angle subtended by the edge of the reflector from the focal point is constant all around the edge. Hence, integration of the incident pattern in any plane from the edge of the reflector to the horizon would give the spillover contribution from the ground. In the clear aperture antenna, due to the asymmetry, the incident pattern on the main reflector is not circularly symmetric. In addition, the angle subtended by the edge of the dish from prime focus varies with the azimuth angle ϕ . The subreflector scattered pattern was calculated in planes at intervals of every 15° in azimuth and a two-dimensional integration of these patterns was carried out to calculate the rear spillover. For the forward spillover also, planes spaced at every 15° were used. Circularly symmetric feed pattern was used in this calculation.

The region past the reflector edge in any plane that is looking into either the ground or the sky depends on the elevation angle of the antenna

and the plane itself. For the rear spillover, to calculate these regions, a reference plane at the prime focus and perpendicular to the central ray from the subreflector to the main reflector was assumed (Figure 2). For the forward spillover, this plane was at the secondary focus and was orthogonal to the feed axis (Figures 3 and 4). Given an elevation angle, for different azimuth angles in the reference plane, the included angle between the reference plane and the horizontal plane (which is parallel to the ground) was calculated. Using this angle, the switchover angle for the spillover going from ground to sky or vice versa in any plane could be determined. Figure 2 shows the orientation of the main reflector for different elevation angles of the antenna. Figures 3 and 4 show the orientation angles of the cassegrain and gregorian subreflectors.

FEATURES OF THE CALCULATIONS:

The spillover calculations were done for a 100-meter main reflector and a 7.2 x 9.8 meter cassegrain subreflector. For the gregorian case, a subreflector of 7.4 x 7.8 meters was used. Figure 1 shows the geometry used in the calculations. A frequency of 1.42 GHz was used. The feed pattern used for the forward spillover had a -12 dB taper at the edge of the subreflector in the cassegrain as well as the gregorian geometry. This same pattern was used in calculating the pattern scattered by the cassegrain subreflector, which in turn was used for the rear spillover computations. The subreflector scattered pattern had about -19 dB taper at the edge of the main reflector which is closer to the subreflector (Figure 1) and about -16 dB taper at the farther edge. It was assumed that the scattered pattern of a gregorian subreflector would be the same as the cassegrain pattern. For the ground a temperature of 270 K was used, and for the sky 6 K was used.

RESULTS:

Results of the spillover computations are shown in Table 1 for elevation angles from 10° to 90°. There are only two columns for the rear spillover, one for the bottom arm and the other for the top arm, as the subreflector patterns for the cassegrain and gregorian are about the same as mentioned elsewhere. At zenith, rear as well as forward spillover for the four cases is the same. From Figure 2a, it is clear that the rear spillover with arm at the top is mainly on the ground for all the elevation angles. The monotonic increase in the rear spillover temperature T_r going from 90° to 10° elevation is due to the fact that the solid angle looking at ground around the -16 dB edge increases while that around the -19 dB edge decreases. The increase in ground pickup around the -16 dB edge is greater than the decrease in pickup around the -19 dB edge. For the arm at the bottom, with decrease in elevation angles, the -16 dB edge travels past the horizon as seen in Figure 2b, thus decreasing the ground contribution while increasing the sky pickup. Hence, T_r decreases at lower elevation angles.

For the cassegrain at the top (Figure 3a), the forward spillover moves from the sky towards the ground with decrease in elevation. At 10° elevation about 80% of the spillover is hitting the ground and hence the

forward spillover temperature T_z is 25 K. If all the spillover hits the ground, T_z is about 32 K. T_z is high due to the shape of the feed pattern which could be approximated by a Gaussian beam. For the arm at the bottom (Figure 3b), the spillover is mostly in the sky and T_z increases by 0.2 K going from zenith to 10° when one edge of the subreflector gets close to the ground. For the gregorian at the top, again most of the spillover is in the sky except at low elevation angles (Figure 4a). At these positions the lower edge has moved closer to the ground than the cassegrain at the bottom, for the same elevation angles and hence T_z is higher. When the gregorian is at the bottom, at 10° elevation about 50% of the spillover is into the ground (Figure 4b). Hence, T_z is high at 16 K.

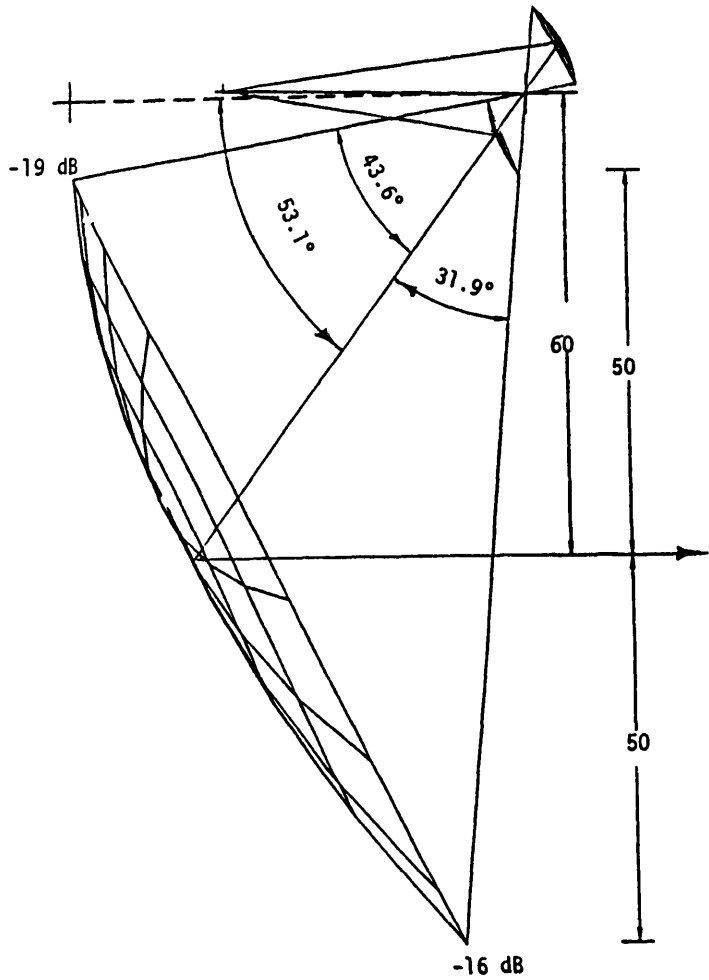
CONCLUSION:

Figures 5 through 7 compare the total spillover for the cassegrain and gregorian cases. Certainly, the cassegrain with arm at the top and gregorian with arm at the bottom can be ruled out. Figure 7 compares the cassegrain at the bottom to the gregorian at the top. The rear spillover component of the total spillover is shown in broken lines. The total spillover of the cassegrain at the bottom is lower for all elevation angles (except at zenith where it is the same as that of the gregorian at the top) and is lower by 2 K at 30° and by 3.5 K at 10° . Changing the illumination taper at the subreflector edge and/or using a flange around the subreflector would decrease the difference. But due to the rear spillover difference, the CASSEGRAIN AT THE BOTTOM would still be BETTER by 1.9 K at 30° and by 2.5 K at 10° elevation.

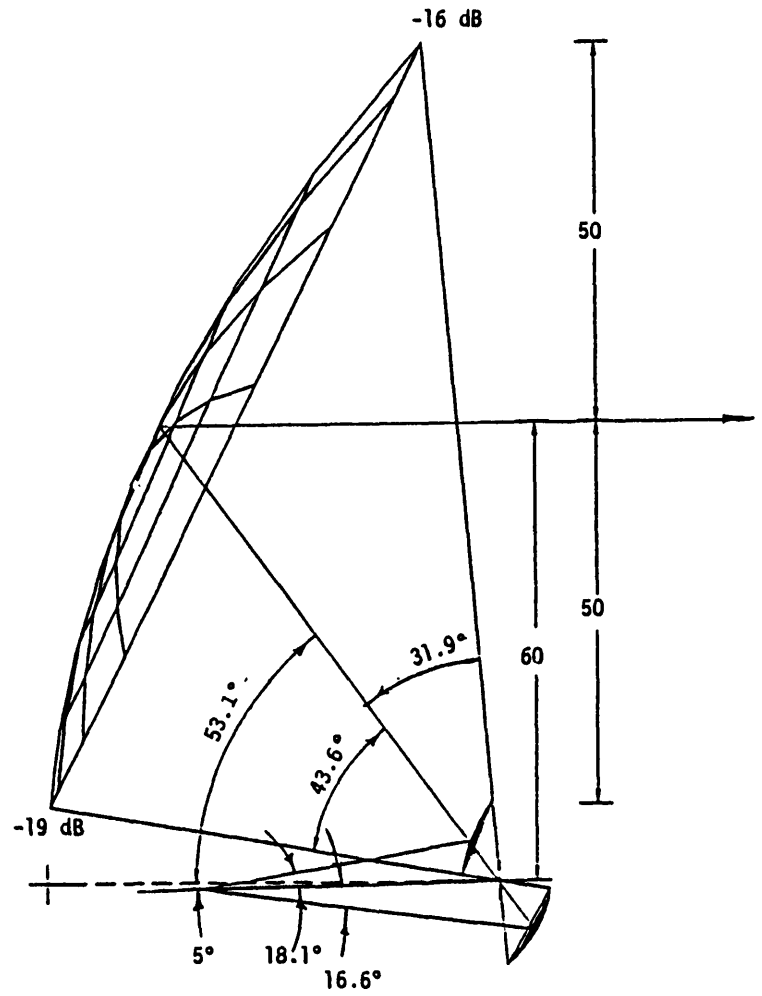
A word of thanks to John Granlund for the useful discussions in arriving at some geometric solutions.

TABLE 1. Spillover Noise Temperatures

ELEVATION	REAR T _r (K)		FORWARD T _f (K)				TOTAL T (K)			
			CASSEGRAIN		GREG		CASSEGRAIN		GREG	
(Degrees)	Bottom	Top	Bottom	Top	Bottom	Top	Bottom	Top	Bottom	Top
90	2.866	2.866	0.650	0.650	0.650	0.650	3.516	3.516	3.516	3.516
75	1.995	3.103	0.595	0.680	0.709	0.607	2.590	3.783	2.704	3.710
60	1.643	3.167	0.586	0.772	0.729	0.672	2.229	3.939	2.372	3.839
45	1.503	3.204	0.641	2.029	0.895	0.721	2.144	5.233	2.398	3.925
30	1.300	3.245	0.679	13.186	2.956	0.744	1.979	16.431	4.256	3.989
20	1.107	3.250	0.754	17.750	10.855	0.940	1.861	21.000	11.962	4.190
10	0.791	3.277	0.860	25.077	15.964	1.843	1.651	28.354	16.755	5.120



(a) Arm at the Top.



(b) Arm at the Bottom.

Fig. 1. Cassegrain, Gregorian Geometry.

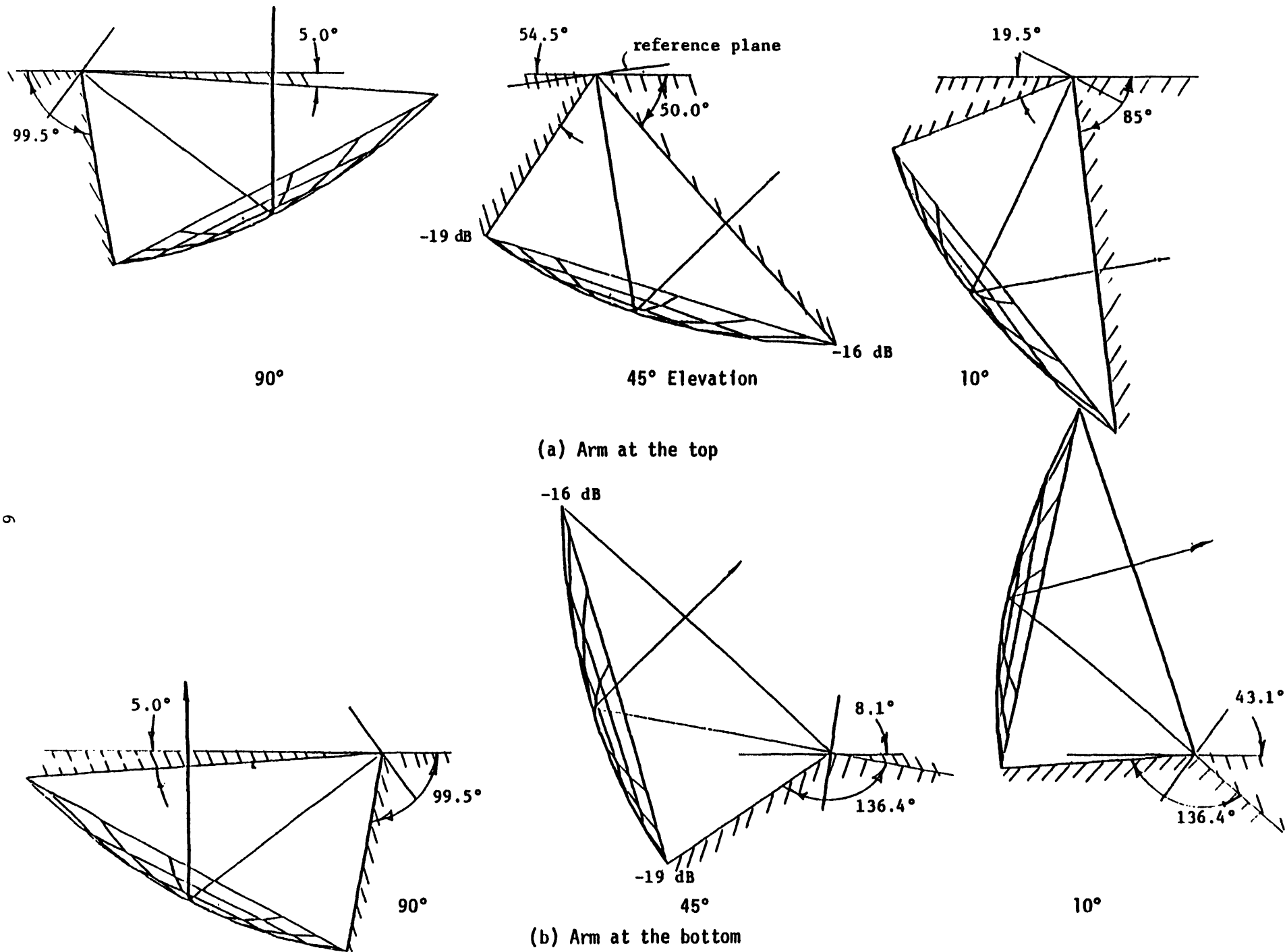
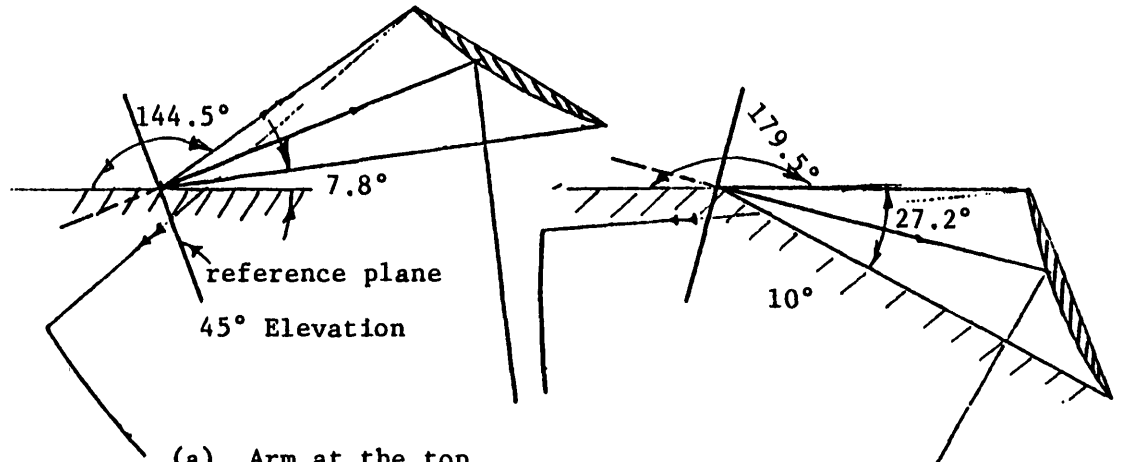
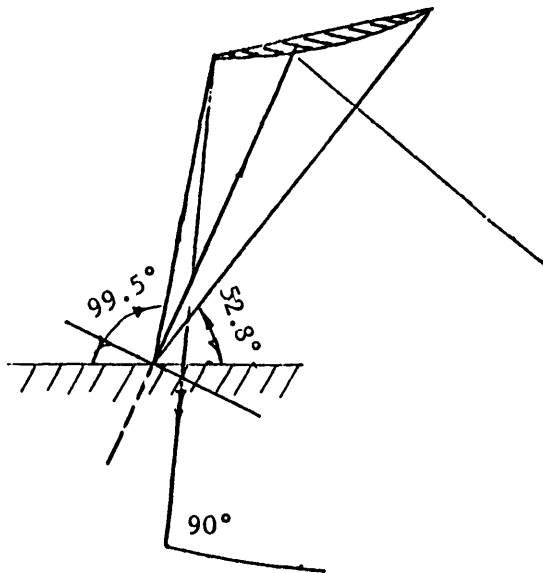
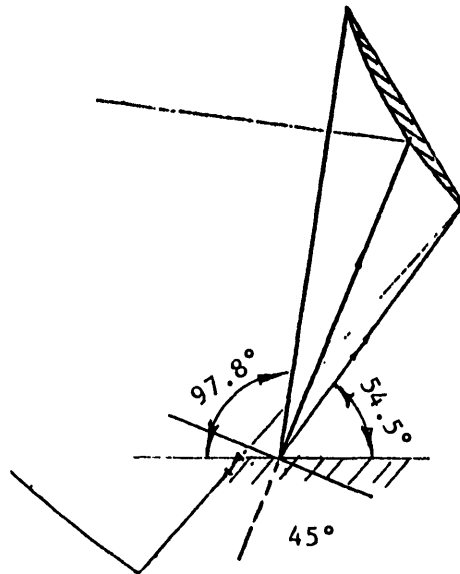
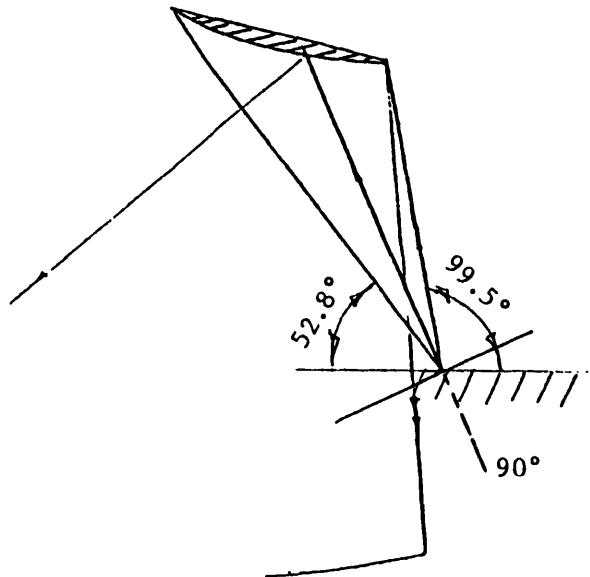


Fig. 2. Rear Spillover. Main Reflector Orientation with Respect to Ground (shaded).



(a) Arm at the top



(b) Arm at the bottom

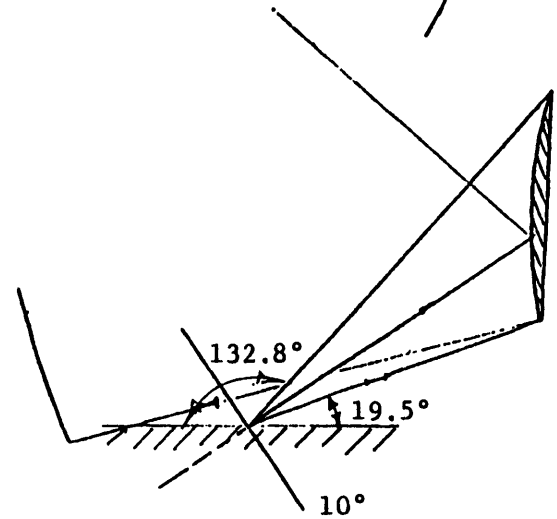
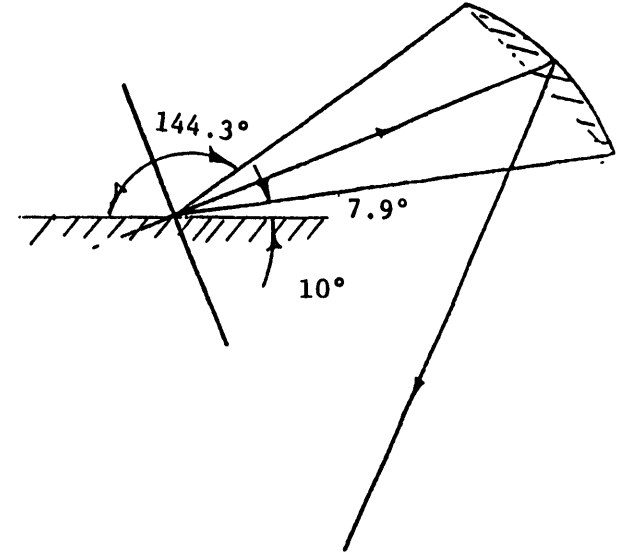
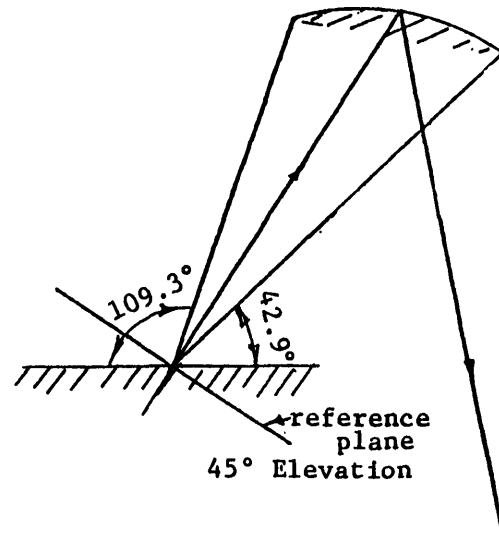
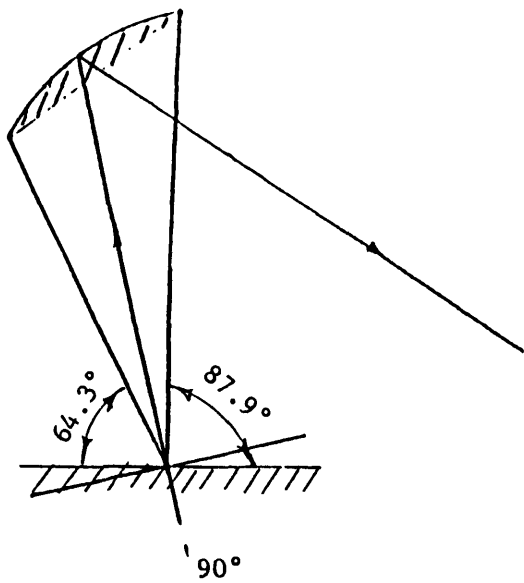
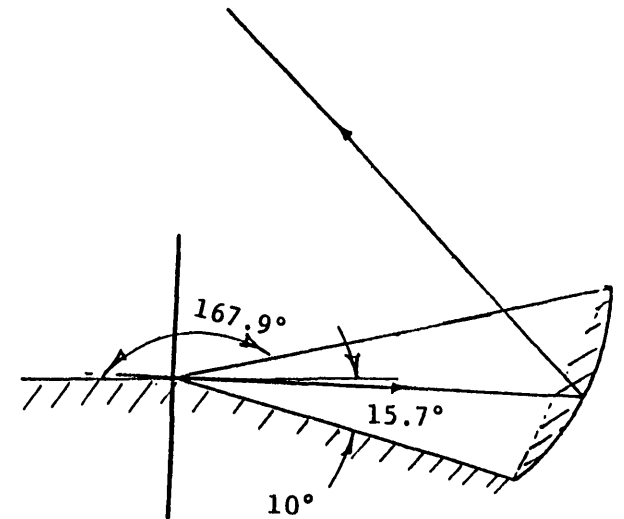
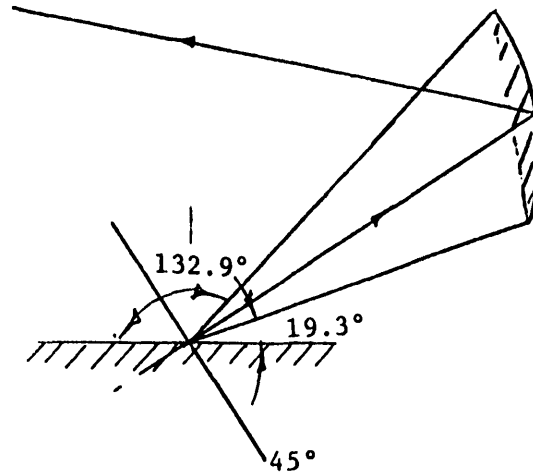
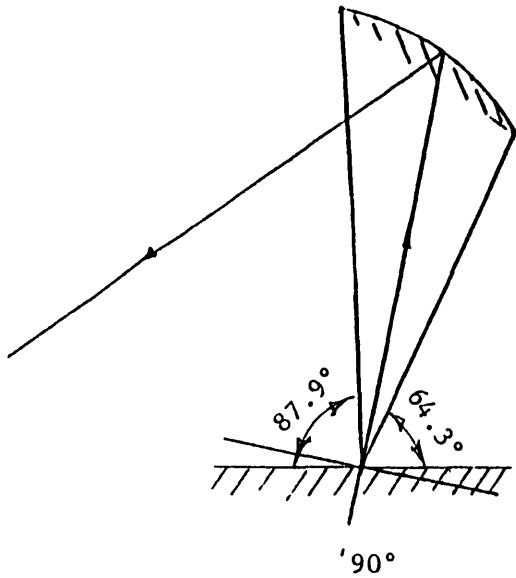


Fig. 3. Forward Spillover. Cassegrain Subreflector Orientation with Respect to Ground (shaded).



(a) Arm at the top



(b) Arm at the bottom

Fig. 4. Forward Spillover. Gregorian Subreflector Orientation with Respect to Ground (shaded).

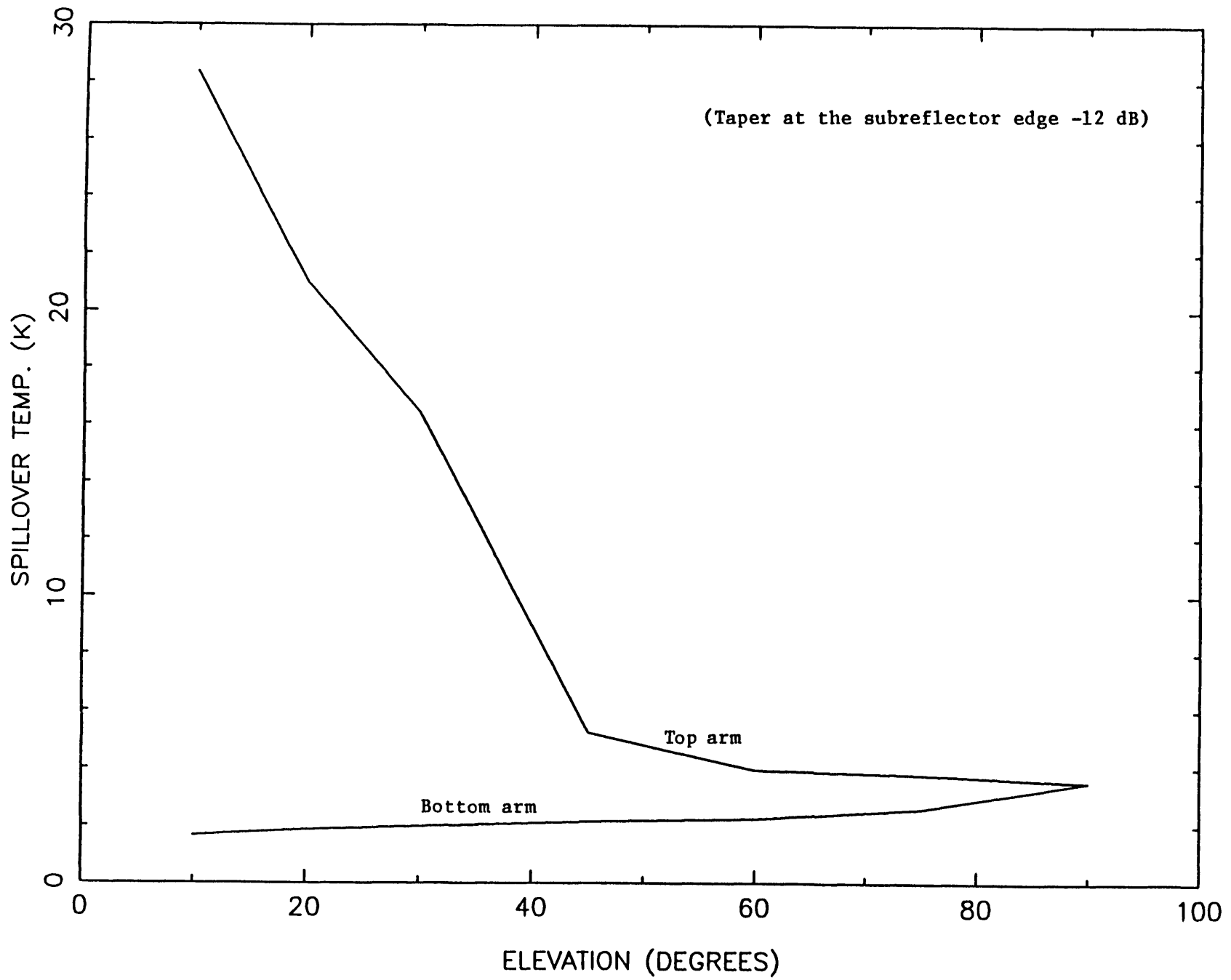


Fig. 5. Total Spillover Noise Temperature (Cassegrain Geometry) - Bottom Arm vs. Top Arm.

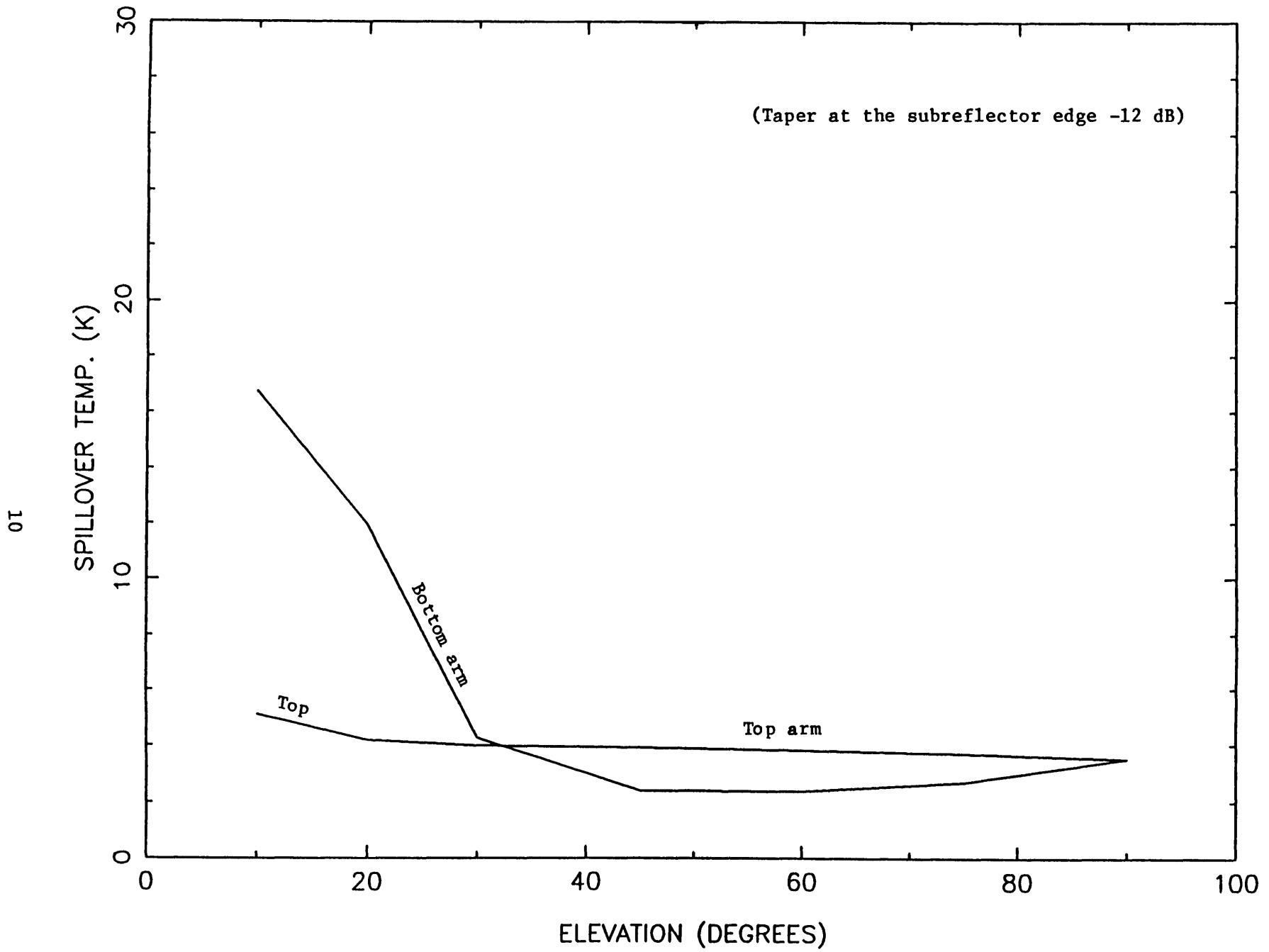


Fig. 6. Total Spillover Noise Temperature (Gregorian Geometry) - Bottom Arm vs. Top Arm.

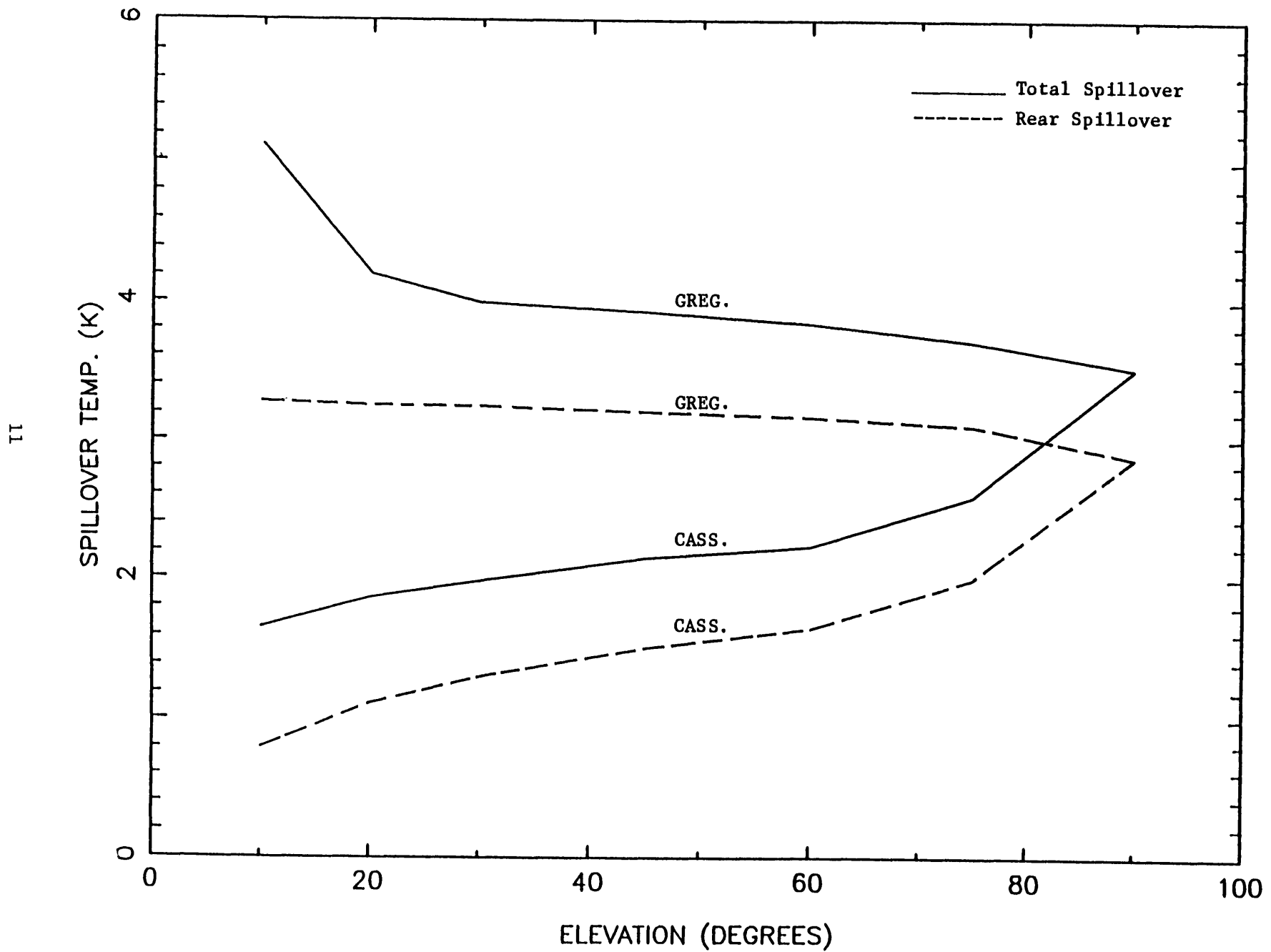


Fig. 7. Spillover Noise Temperature - Cassegrain at the Bottom (Cass.) vs. Gregorian at the Top (Greg.).